Supplement of Atmos. Chem. Phys., 23, 8823–8835, 2023
https://doi.org/10.5194/acp-23-8823-2023-supplement

Atmospheric Chemistry and Physics
Open Access
EGU

Supplement of

Can we use atmospheric CO_2 measurements to verify emission trends reported by cities? Lessons from a 6-year atmospheric inversion over Paris

Jinghui Lian et al.

Correspondence to: Jinghui Lian (jinghui.lian@suez.com)

This PDF file includes:

Supplementary text S1 to S4

Figures S1 to S13

Table S1

SI References

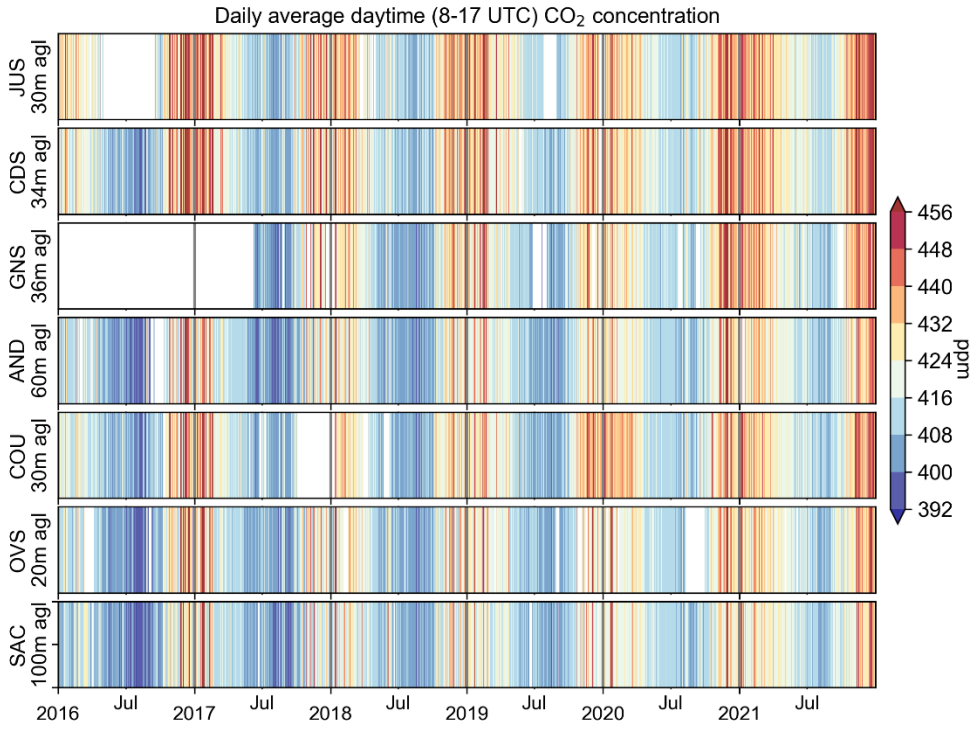

Figure S1. Daily average daytime (8-17 UTC) observed CO_2 concentrations from 2016 to 2021 at seven in situ stations within Paris and its surrounding areas, together with their respective heights above ground level of the air intake inlet.

Text S1. Origins.earth fossil fuel CO_2 emission inventory

The Origins.earth inventory compilation method is mainly based on methodologies developed by Pôle National des Inventaires Territoriaux (PCIT, 2019), the body tasked by the French government to establish national guidelines for computing GHG emission inventories for local authorities. The near real-time high-resolution CO_2 emission maps are generated through the following two-step process. The first step involves the construction of gridded annual CO_2 emission datasets for different sectors for the base year 2018, which consists in spatializing geographically the intensity of annual emissions of the IdF region reported by the French climate agency (ROSE, https://www.roseidf.org/). Sector-specific spatial proxies (i.e., high spatial resolution French population census, CORINE Land Cover, locations of the thermal power stations, incinerators, and main emitting industries) are applied to allocate emissions to spatially resolved grids. The second step combines the annual sectorial emission maps with respective generic and/or measure-based (real activity data) temporal profiles. It combines the annual sectorial emission maps with respective generic and/or measure-based (real activity data) temporal profiles. For example, the on-road traffic emissions in the city of Paris are scaled using the real-time traffic count data from more than 3000 traffic measurement points. For the on-road traffic outside the Paris city, the temporal variations are assumed to follow the mean changes of the ones in the city. The temporal evolution of the residential emissions is estimated using the domestic gas consumption data from the SmartGRT database (https://smart.grtgaz.com/en/consommation). This proxy discards the specific temporal variations of other energy sources for the residential sector (e.g., petroleum, wood, coal), which may introduce additional uncertainties. Emissions from the tertiary, industry and energy are downscaled to hourly values based on the industrial gas consumption without SFM (Sites Fortement Modulés). Note that developing the near real-time CO_2 gridded emissions by sector at high-resolution is a relatively new endeavor. We continue to revise the methodology to further improve data quality.

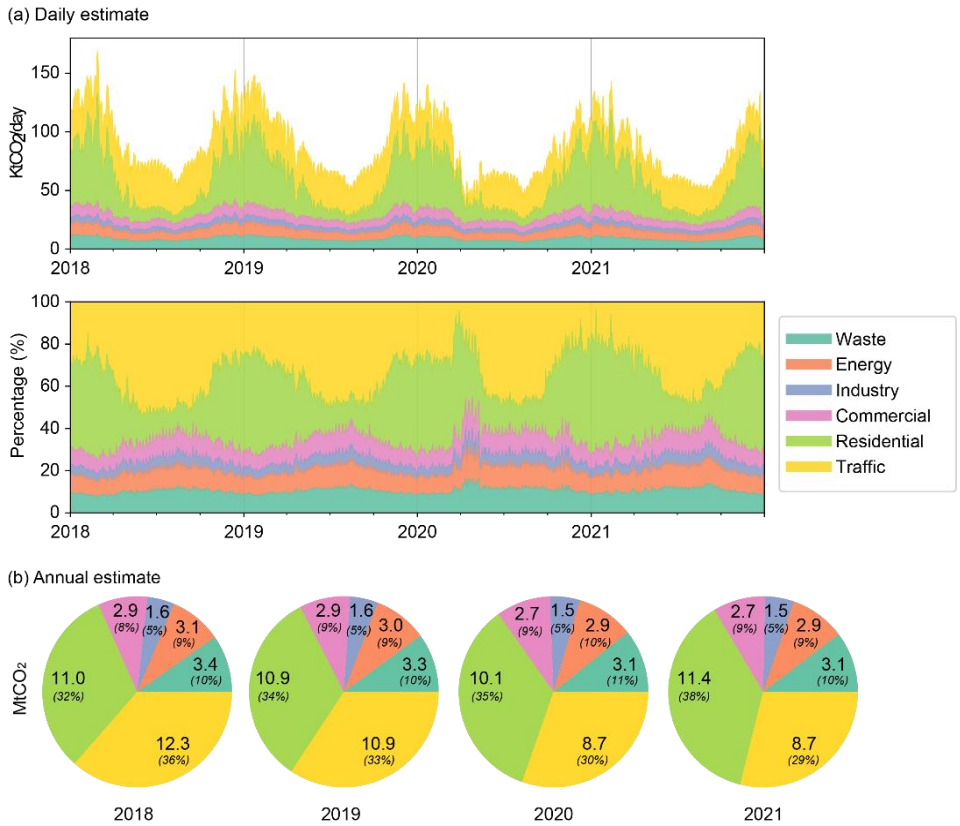

Figure S2. (a) Daily and (b) annual sectorial fossil fuel CO_2 emission estimates and their respective proportions from 2018 to 2021 according to the Origins.earth inventory.

Text S2. Evaluation of the observed and modeled ABL heights

In this study, we assume systematic differences between the thermodynamic and aerosol-based layer detection are negligible or in fact that the aerosol-based results provide a more suitable description for the dilution of near-surface CO_2 emissions, but it should be noted that these issues are subject to current research (Kotthaus et al. 2023).

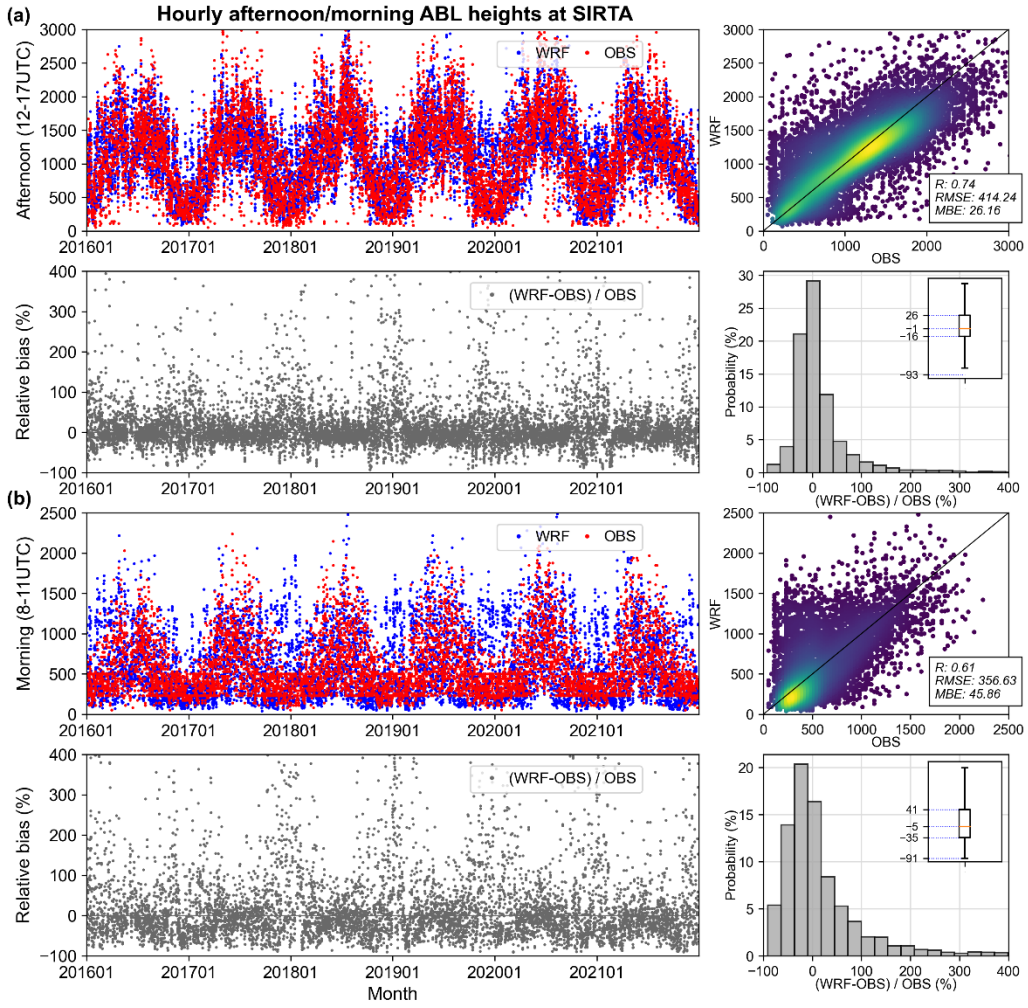

Figure S3. Comparison of the observed and modeled hourly ABL heights at SIRTA station, both for the (a) afternoon (12-17 UTC) and (b) morning (8-11 UTC) period.

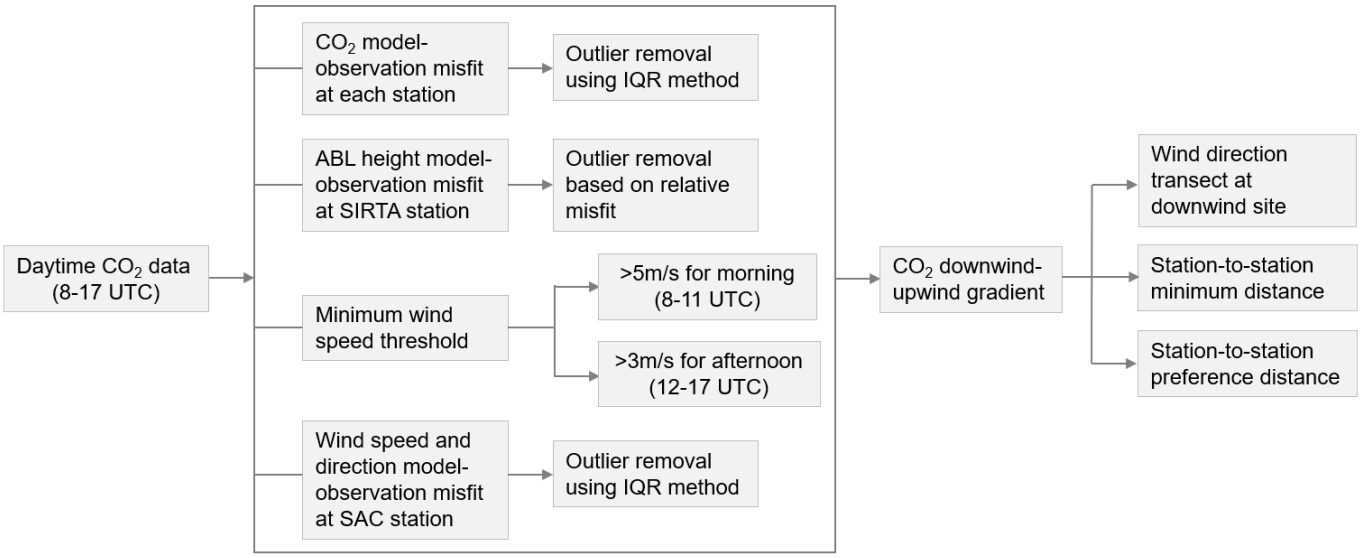

Figure S4. Roadmap for the selection of the assimilated CO_2 observation data into the inversion system

Table S1. Summary of inversion configurations used in this study, both for the reference inversion setup and for the sensitivity tests with changing one configuration at a time compared to the reference.

Category	Description	Reference inversion	Sensitivity test
Data selection criteria	Time period of the assimilated data	Daytime (8-17 UTC)	Morning (8-11 UTC) / Afternoon (12-17 UTC)
	Wind bias outlier based on an interquartile range (IQR) method	0.5	
	Minimum wind speed	3m/s	
	Wind direction transects	30°	20°
	Station-to-station minimum distance	10km	
	Station-to-station preference distance	32 km	20km / 40 km
Prior flux uncertainty	Day-to-day temporal correlation	1 day	4 days
	Uncertainty for 6h fossil fuel flux	60%	40% / 80%
	Uncertainty for daily biogenic flux	60%	40% / 100%

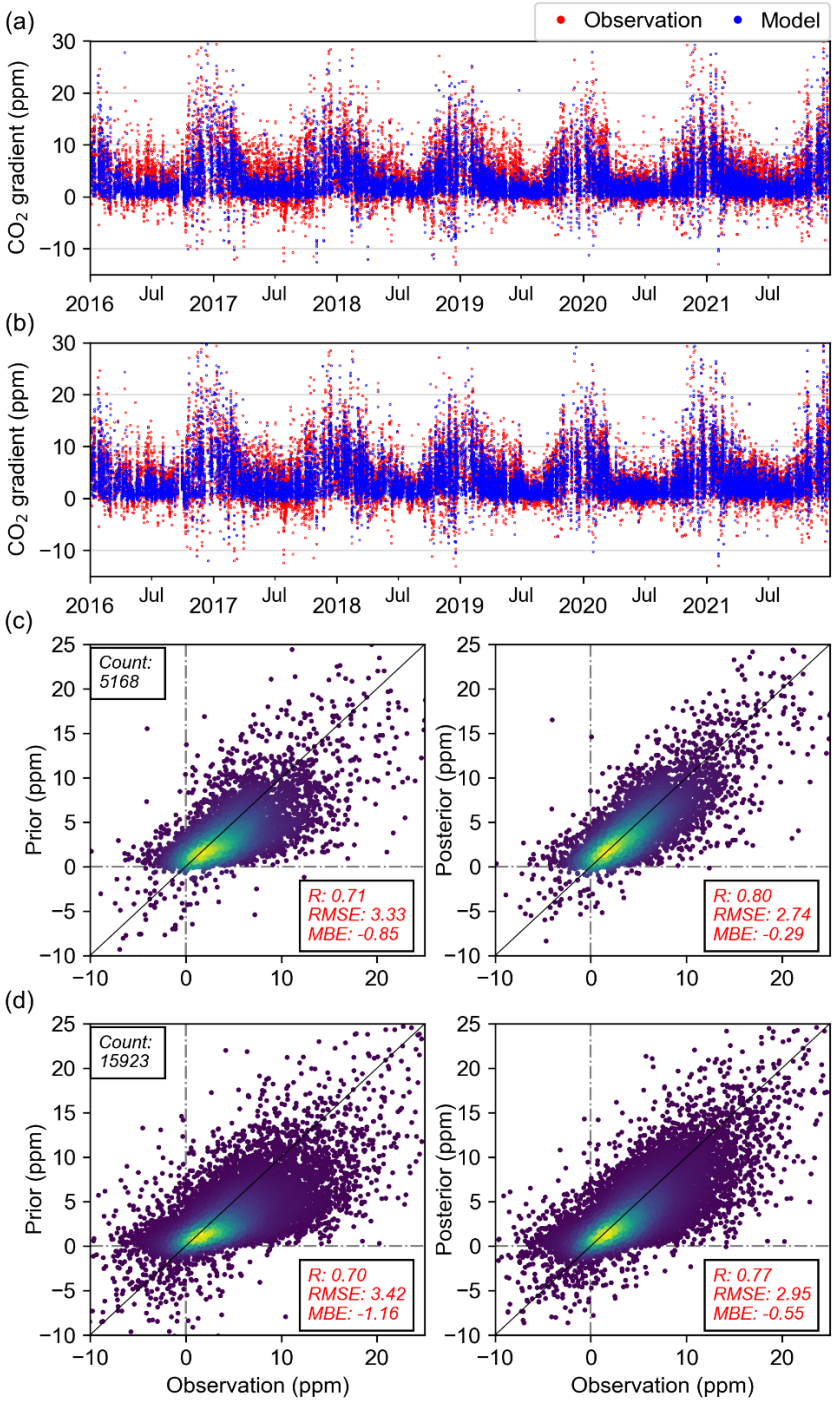

Figure S5. The assimilated hourly daytime CO_2 concentration gradients with (a) prior fluxes and (b) posterior fluxes against the observations from 2016 to 2021. Scatter plot of the assimilated observations and the corresponding simulated CO_2 concentration gradients using the prior fluxes and the posterior fluxes for the (c) morning 8-11 UTC and (d) afternoon 12-17 UTC period, respectively. The statistics of the coefficient correlation (R), root mean square error (RMSE) and mean bias error (MBE) of prior model-data misfit and posterior model-data misfit for the inversion are also provided in the figure.

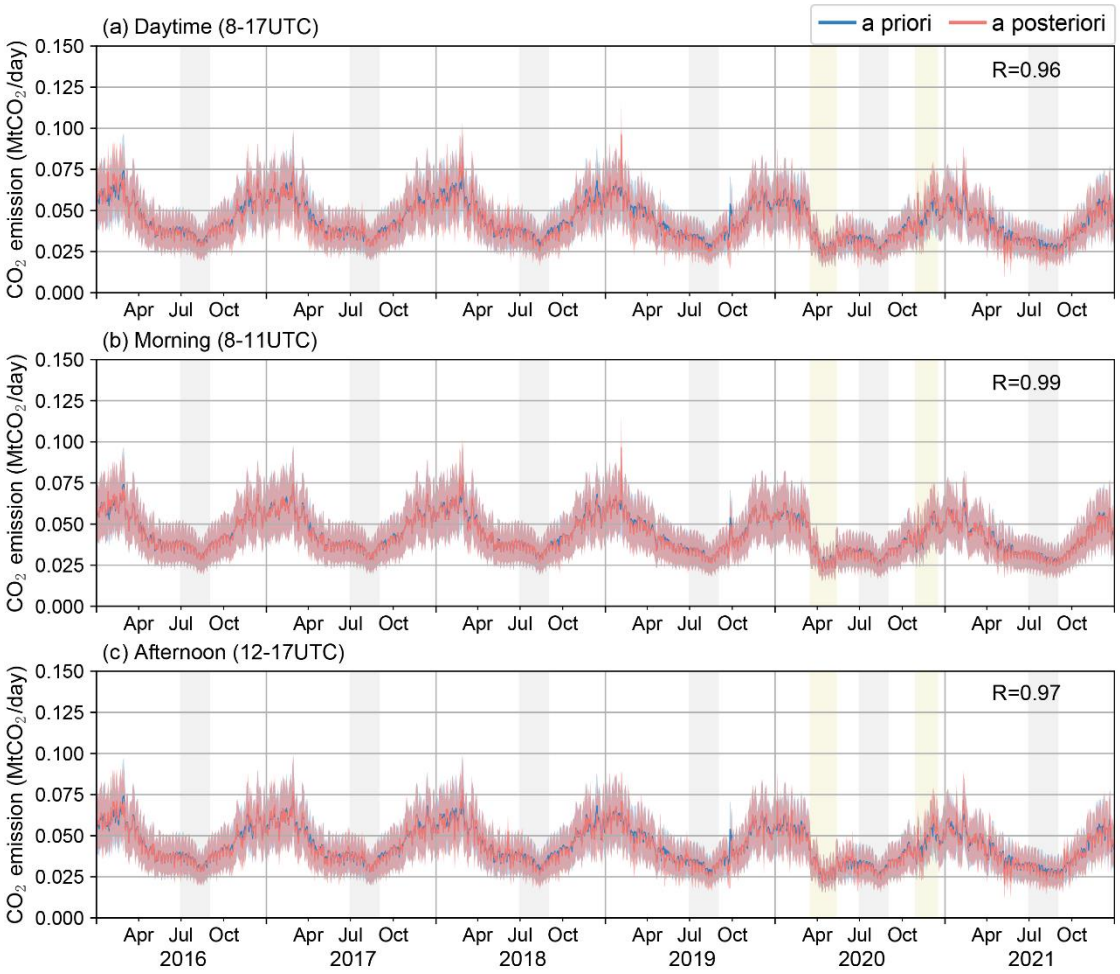

Figure S6. Daily estimates of fossil fuel CO_2 emissions over the rest of IdF region when assimilating (a) daytime (8-17UTC), (b) morning (8-11UTC) and (c) afternoon (12-17UTC) CO_2 concentration observations. The blue line and shading show the prior flux according to the Origins.earth inventory together with its assumed uncertainty. The pink and shading show the posterior estimates with their uncertainty ranges. The yellow shaded areas are the two COVID-19 lockdown periods in France. The grey shaded areas are the summer holidays of July and August.

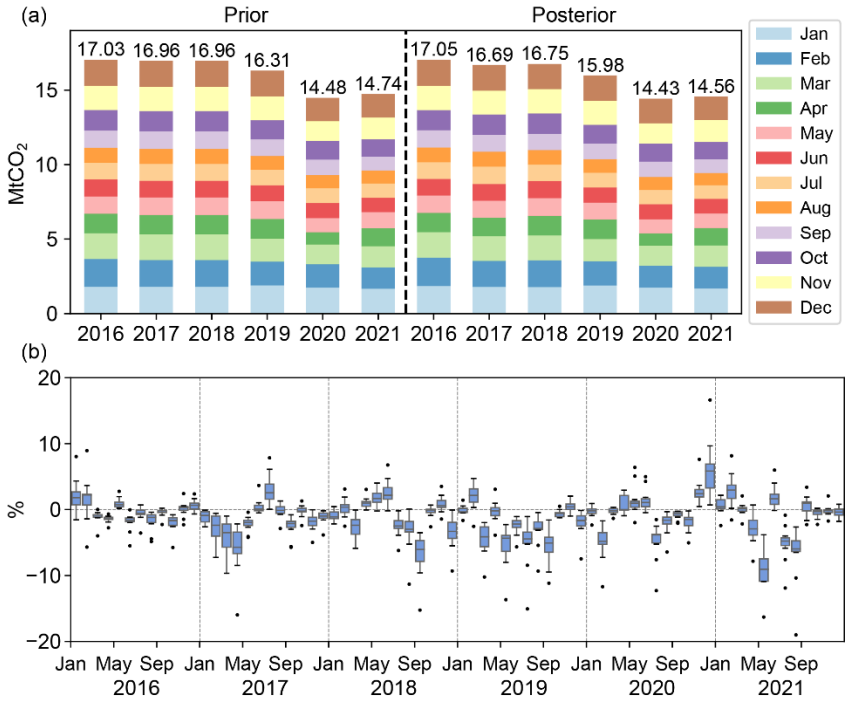

Figure S7. (a) Prior and posterior estimates of the monthly total fossil fuel CO_2 emission over the rest of IdF region. (b) the change of CO_2 emissions in percentage (posterior-prior)/prior. The boxplots are the posterior emissions from an ensemble of sensitivity tests of the inversion configuration.

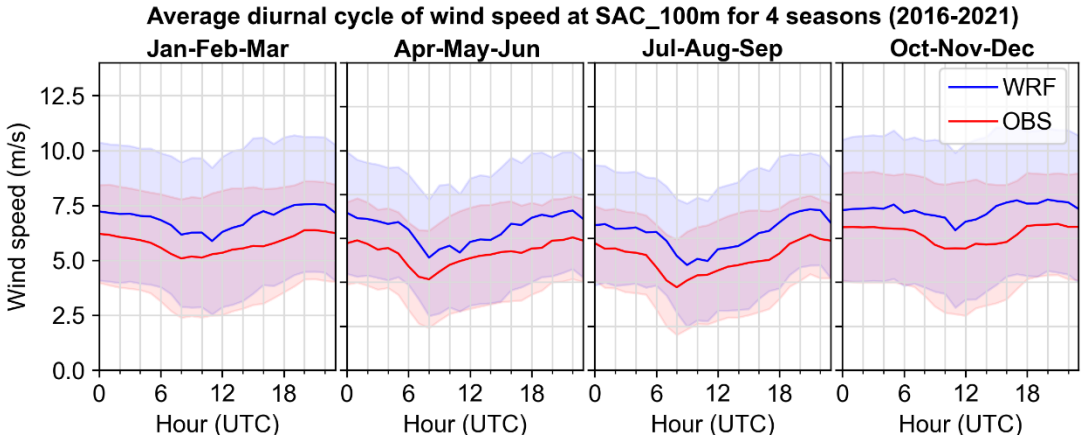

Figure S8. Average diurnal cycle and the standard deviation of the observed and modeled wind speeds at 100m above the ground level at SAC station for four seasons from 2016 to 2021.

Text S3. Residential heating

Residential CO_2 emissions are typically determined by multiple energy consumption statistics accounting for fossil fuels and their corresponding emission factors. It usually includes petroleum, bottle gas, city gas, wood, and coal. Note that the electricity and urban network energy sources are included in the energy sector in the Origins.earth inventory and are therefore not accounted for here. The calculation of fossil fuel CO_2 emissions for the residential sector in the Origins.earth inventory follows two steps: (1) estimating the spatialized annual emissions from different energy consumption sources. (2) downscaling annual emission to the hourly time scale based on the domestic gas consumption data from the SmartGRT database (https://smart.grtgaz.com/en/consommation). This assumption of the evolution of emissions with time ignores the temporal variations of other energy sources for the residential sector (e.g., petroleum, wood, coal). We thus calculate the proportions of annual residential fossil fuel CO_2 emissions from different energy types (Figure S9). These shares indicate that the temporal variation of residential CO_2 emissions from petroleum and wood burning might be an important missing source in the Origins.earth inventory, especially in suburban areas.

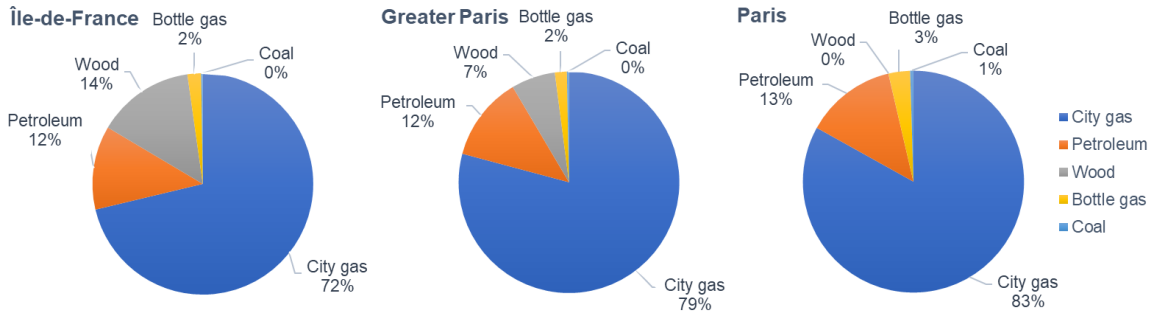

Figure S9. The proportions of annual residential fossil fuel CO_2 emissions from different energy types (in percentage) over Île-de-France, Greater Paris and Paris city respectively.

Text S4. Biogenic flux

The VPRM modeled biogenic fluxes (net ecosystem exchange, NEE) are compared with the eddy flux measurements at two stations within the IdF region (Figure S10). The Fontainebleau forest site (48.4763°N; 2.7801°E) is located southeast of Paris center. Deciduous broadleaf trees (oak (Quercus petraea and Quercus robur), beech (Fagus sylvatica), and hornbeam (Carpinus betulus)) are the dominant species in the vicinity of the flux tower. The Grignon site (48.8442°N, 1.9519°E) is located at around 40 km west of Paris. The crop is a maize, winter-wheat, oilseed rape, winter-wheat rotation.

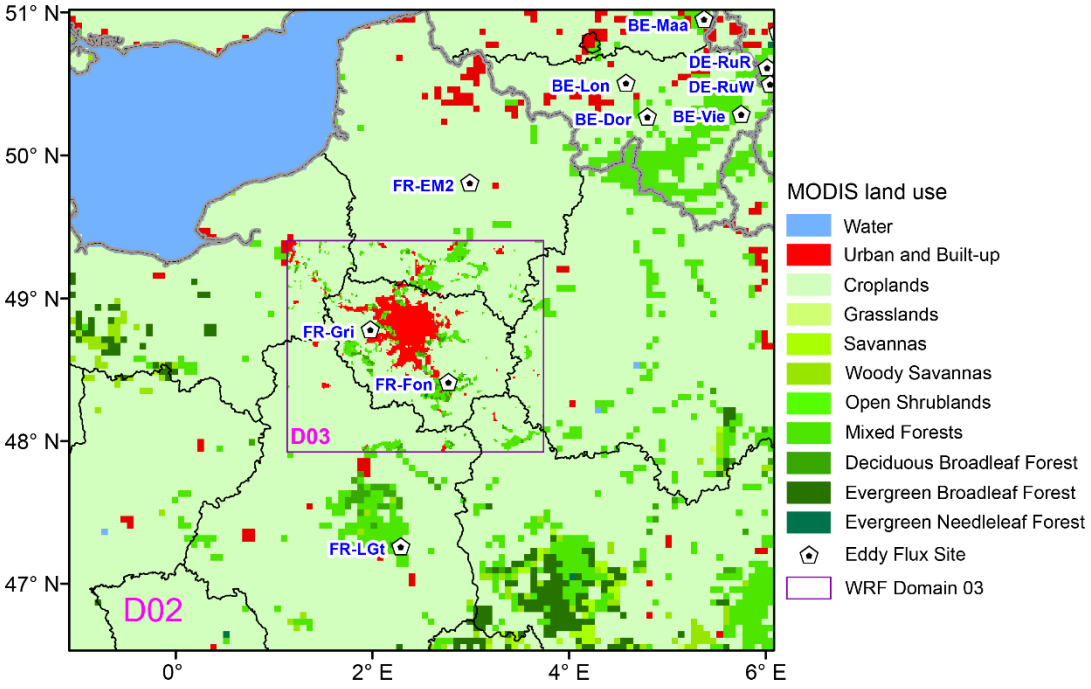

Figure S10. Locations of eddy flux stations within the inner two WRF domains (D02 and D03) together with the MODIS land use map.

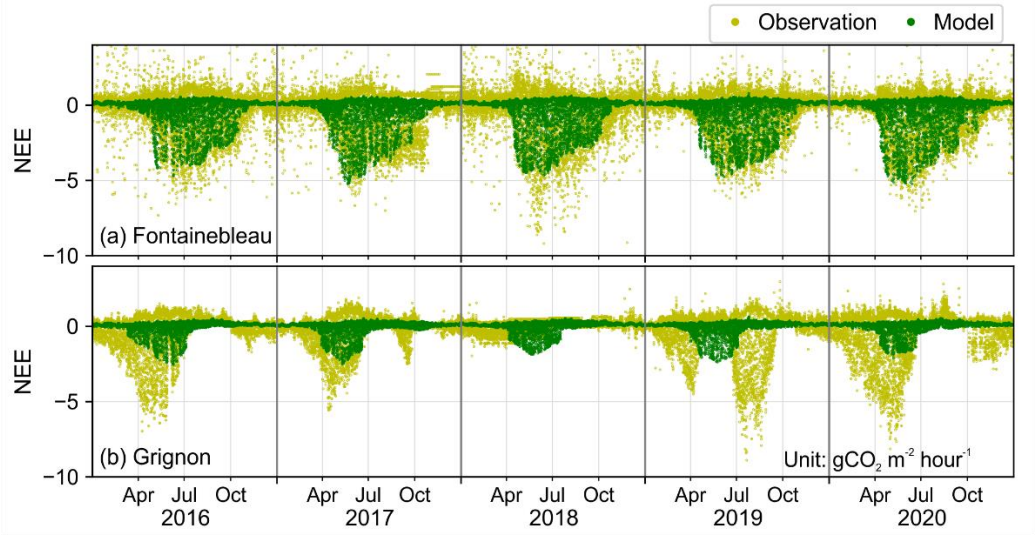

Figure S11. Comparison of the WRF-VPRM simulated hourly biogenic flux (net ecosystem exchange, NEE) with the measured eddy flux data at the (a) Fontainebleau forest station and (b) Grignon cropland station from 2016 to 2020.

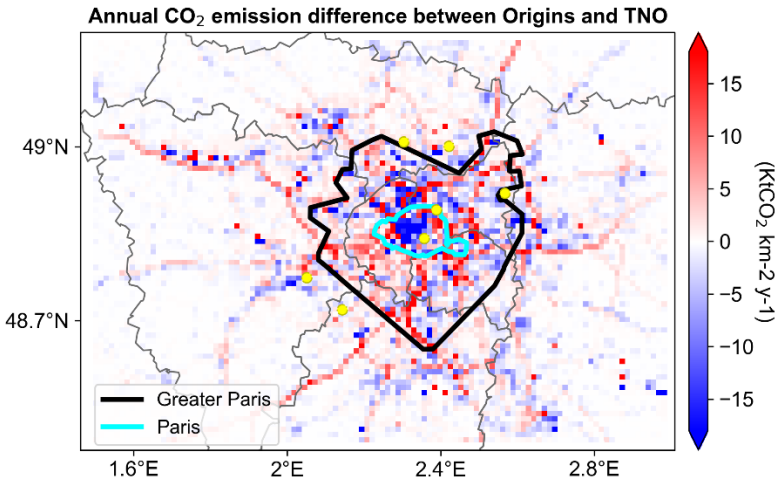

Figure S12. Differences in annual fossil fuel CO_2 emission between the Origins.earth and the TNO 1km inventory for the year 2018.

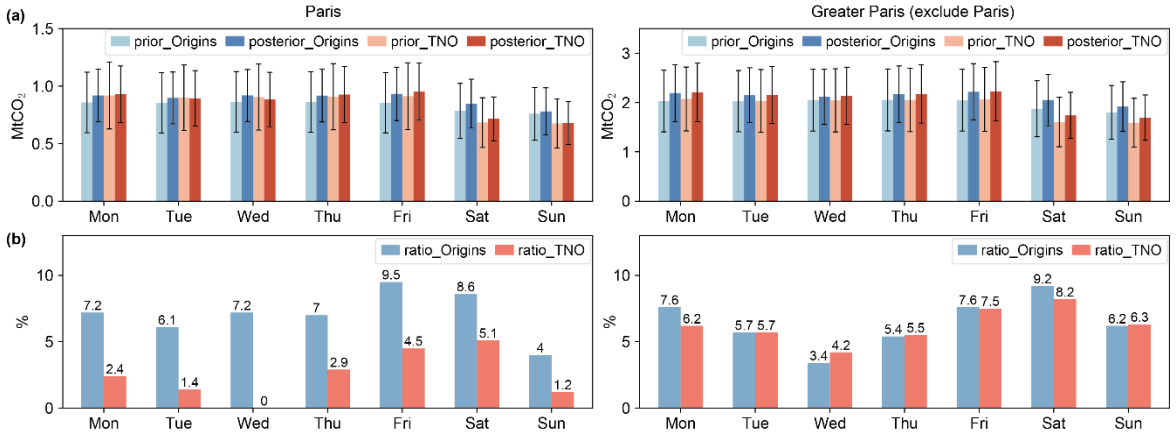

Figure S13. (a) Annual fossil fuel CO_2 emissions prior estimates by Origins.earth and TNO 1km inventory and the respective posterior estimates for the seven days of the week in 2018 over the city of Paris (left panel) and the rest of Greater Paris region (right panel) (cf. Figure S12) respectively. (b) the change of CO_2 emissions in percentage (posterior-prior)/prior.

SI References

Kotthaus, S., Bravo-Aranda, J. A., Collaud Coen, M., Guerrero-Rascado, J. L., Costa, M. J., Cimini, D., O'Connor, E. J., Hervo, M., Alados-Arboledas, L., Jiménez-Portaz, M., Mona, L., Ruffieux, D., Illingworth, A., and Haeffelin, M.: Atmospheric boundary layer height from ground-based remote sensing: a review of capabilities and limitations, Atmos. Meas. Tech., 16, 433–479, https://doi.org/10.5194/amt-16-433-2023, 2023.

Lian, J., Lauvaux, T., Utard, H., Broquet, G., Bréon, F.M., Ramonet, M., Laurent, O., Albarus, I., Cucchi, K., and Ciais, P.: Assessing the Effectiveness of an Urban CO_2 Monitoring Network over the Paris Region through the COVID-19 Lockdown Natural Experiment. Environmental Science & Technology, https://doi.org/10.1021/acs.est.1c04973, 2022.

Pôle de Coordination des Inventaires Territoriaux, Guide méthodologique pour l'élaboration des inventaires territoriaux des émissions atmosphériques, 2018, Ministère Chargé de l'Environnement. Available online: https://www.lcsqa.org/system/files/media/documents/MTES_Guide_methodo_elaboration_inventaires_PCIT_mars2019.pdf (accessed on 17 March 2022).